CHAPTER 4
RESULTS AND DISCUSSION

4.1 Autocorrelations and cross-correlations of variables

The autocorrelation of a variable and the cross-correlation between two variables are important factors to consider for modeling purposes. The effects of wind speed, global solar radiation and temperature might be highly auto-correlated or closely interrelated for up to 24 hr. The auto-correlation function (ACF) plot, as discussed earlier will indicate the time-dependence of a variable with its past values. The plots in Figure 4.1 are based on the dataset for the period 2001-2006, for the months of March and August, as an example. The sample ACF of the detrended data for the wind speed (*S*), global solar radiation (*GR*), vertical temperature difference (*VTD*), and land-sea temperature difference (*LSTD*) shows that this pattern is apparent in all the variables considered. Wind speed shows relatively more positive autocorrelations at a high number of lags compared to the other variables. On the other hand, global solar radiation, vertical temperature difference and land-sea temperature difference have a number of positive autocorrelations up to the sixth lag, upon which the autocorrelations become negative before cycling back to positive values. As mentioned earlier, sample autocorrelation function (ACF) of the detrended data exhibit peaks of the autocorrelations at an interval of 24 hours, indicative of a diurnal cycle. This indicates that observations that are 24 hours apart are positively correlated for all the variables considered.

A plot of the cross-correlation function (CCF) is used to show if any two variables are interdependent, with the lead-lag relationship identifying the predictor for the main variable (Cowpertwait and Metcalfe, 2009). Figure 4.2 shows CCF plots for detrended data. In Figures 4.2 (a) and (d), the wind speed and global solar radiation have several higher values for the cross-correlation at negative lags (up to 7), indicating that the leading variable is the global solar radiation, and therefore, it is an important predictor of wind speed. On the other hand, the CCFs of vertical temperature difference, and land-sea temperature difference relative to wind speed exhibit a feedback relationship being mostly symmetrical around lag zero (h) for August, as seen in Figure 4.2 (e, f) whereas for March, a higher level of positive correlations appear on the negative lags for land-sea

temperature difference with respect to wind speed. This behavior was also seen in the other monthly series (not shown). Therefore, it would be important to capture the autocorrelations and cross-correlations by using a suitable multivariate model. Table 4.1 shows the correlation among detrended values of variables considered for the VAR model based on the training period spanning 2001-2004. The wind speed is seen to have higher correlation with the vertical temperature difference and land-sea temperature difference at 0.29 and 0.15 respectively, when compared to that between the wind speed and global solar radiation (0.09). Also considering the fact that global solar radiation and vertical temperature difference are both proxies for stability in the boundary layer, and given their relatively high correlation (0.67), it would be sufficient to select either one for the VAR model. Thus, the variables in the final VAR model will be wind speed, vertical temperature difference and land-sea temperature difference.

4.2 Fitted models

The steps outlined in the previous sections helped to identify suitable univariate and multivariate models for all months for wind speed, and wind speed/vertical temperature difference/land-sea temperature difference respectively for the period 2001-2006 (see Table 4.2). Table 4.3 shows the information criterion used for picking the optimal set of models for the ARIMA class of models. It can be seen that the difference between the values for specific models within a particular month based on the *AIC* are minimal. In order to validate if the univariate ARIMA and VAR models captures well the dynamic mechanism of wind speed and its interaction with the other variables, the next section will provide the analysis of fitted time series.

Upon fitting the model to the data, residual diagnostics are performed for the fitted wind speed time series. As discussed earlier for the univariate models, the plot of residuals against time is to check for zero mean and constant variance of the residuals, and the Q-Q plot of residuals is to check the assumption of normally distributed patterns. Figures 4.3-4.10 show the residual diagnostics of the selected models for the months of March and August. It can be seen from the figures that the behavior of the residuals of the selected models fairly agrees with the underlying model assumption and show the goodness-of-fit of the models. Such was the case for the other months and models (not shown).

Further, in considering if the fitted time-series captures the nature of the wind speed, the probability density functions and sample autocorrelations of the actual and fitted time series are plotted for the time span of 2001-2006. The annual mean probability density function plot shows that the VAR model (see, Figure 4.11 (g)) is able to produce the underlying structure of the data, as compared to the others. The other time-series models are also to follow the distribution of the data reasonably. For the sample ACF, all the models show similar patterns, closely matching the time dependence in the real data.

(Intentionally left blank)

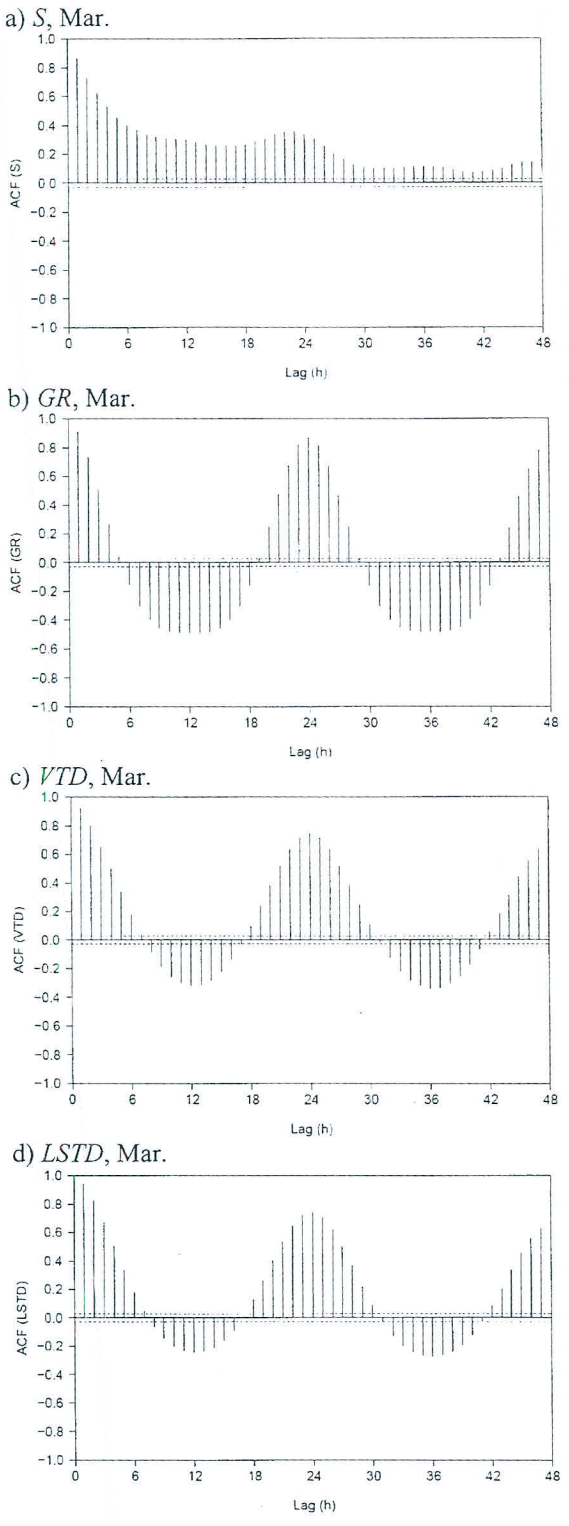

(continued on the next page)

Figure 4.1: ACF: (a) detrended wind speed (*S*), (b) global solar radiation (*GR*), (c) vertical temperature difference (*VTD*), and (d) land-sea temperature difference (*LSTD*) over 2001-2006

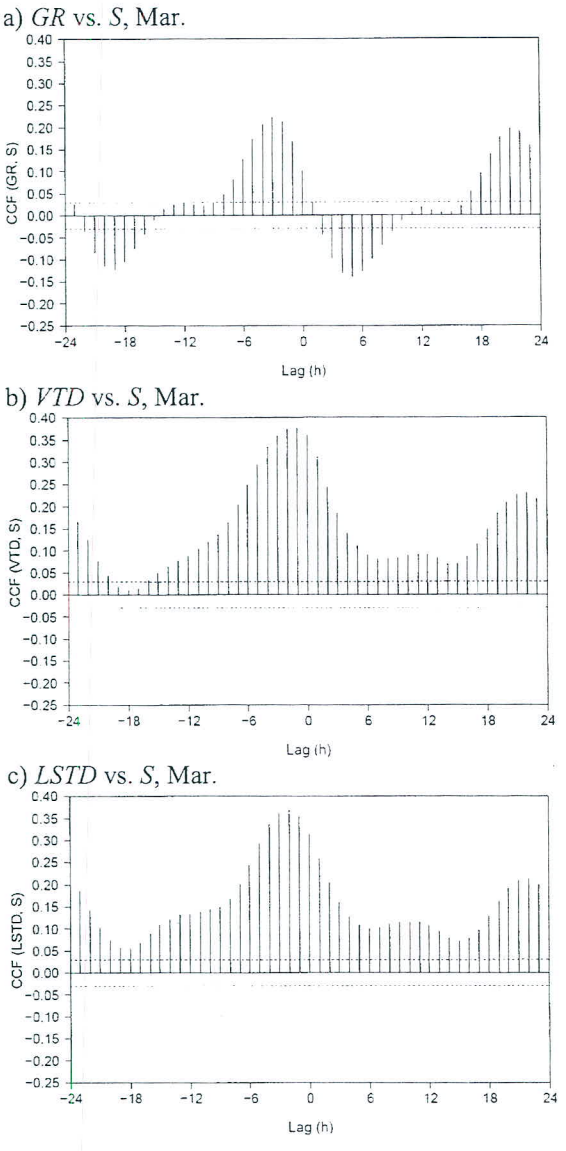

(continued on the next page)

Figure 4.2: CCF of detrended wind speed (*S*) and (a) global solar radiation (*GR*), (b) vertical temperature difference (*VTD*), and (c) land-sea temperature difference (*LSTD*) over 2001-2006

d) *GR* vs. *S*, Aug.

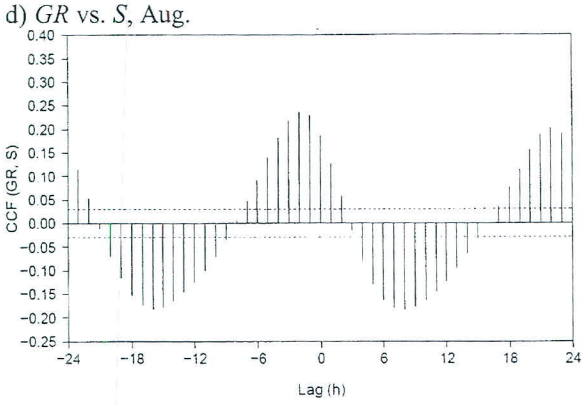

e) *VTD* vs. *S*, Aug.

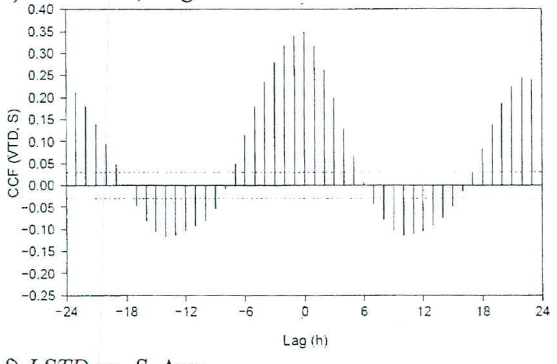

f) *LSTD* vs. *S*, Aug.

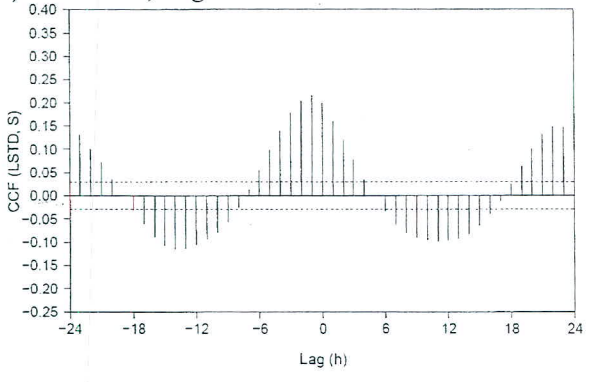

Figure 4.2: (Continued)

Table 4.1: Correlations among the variables considered over 2001-2004

Variables	Correlation
Wind speed (*S*) and global solar radiation (*GR*)	0.09
Wind speed (*S*) and vertical temperature difference (*VTD*)	0.29
Wind speed (*S*) and land-sea temperature difference (*LSTD*)	0.15
Global solar radiation (*GR*) and vertical temperature difference (*VTD*)	0.67
Global solar radiation (*GR*) and land-sea temperature difference (*LSTD*)	0.65
Vertical temperature difference (*VTD*) and land-sea temperature difference (*LSTD*)	0.75

Table 4.2: Selected time-series models

Month	(p, d, q) in ARIMA	(p,d, q) in dARIMA	$(p, d, q)\times(P, D, Q)$ in SARIMA	(p) in VAR
Jan.	(2, 1, 3)	(2, 1, 1)	(2, 1, 1)×(1, 0, 1)	3
Feb.	(2, 0, 1)	(1, 0, 1)	(1, 0, 1)×(1, 0, 1)	3
Mar.	(3, 0, 2)	(1, 1, 1)	(1, 1, 2)×(0, 0, 1)	2
Apr.	(1, 1, 3)	(2, 1, 1)	(2, 1, 1)×(1, 0, 0)	5
May	(2, 1, 2)	(2, 1, 2)	(2, 1, 1)×(1, 0, 1)	2
Jun.	(2, 1, 2)	(2, 1, 1)	(2, 1, 1)×(1, 0, 1)	2
Jul.	(1, 1, 1)	(1, 1, 1)	(1, 1, 1)×(0, 0, 1)	5
Aug.	(2, 1, 3)	(2, 1, 1)	(2, 1, 1)×(1, 0, 0)	2
Sep.	(3, 0, 0)	(3, 0, 1)	(3, 0, 0)×(1, 0, 0)	3
Oct.	(4, 0, 1)	(2, 1, 1)	(2, 1, 1)×(0, 0, 1)	2
Nov.	(1, 0, 4)	(3, 1, 0)	(2, 1, 0)×(1, 0, 0)	2
Dec.	(2, 1, 3)	(1, 1, 2)	(2, 1, 1)×(1, 0, 1)	4

Table 4.3: AIC for the selected models

Month	AIC		
	ARIMA	dARIMA	SARIMA
Jan.	2628.0	2557.9	2568.9
Feb.	4361.4	4238.5	4281.5
Mar.	625.2	618.0	626.9
Apr.	1115.4	1078.4	1110.4
May	691.6	678.6	691.5
Jun.	1120.7	1089.3	1110.3
Jul.	691.8	678.1	691.1
Aug.	1046.7	1016.7	1045.3
Sep.	676.2	657.8	676.2
Oct.	1011.3	1004.3	992.0
Nov.	1019.2	1010.8	1033.9
Dec.	2251.2	2177.4	2222.5

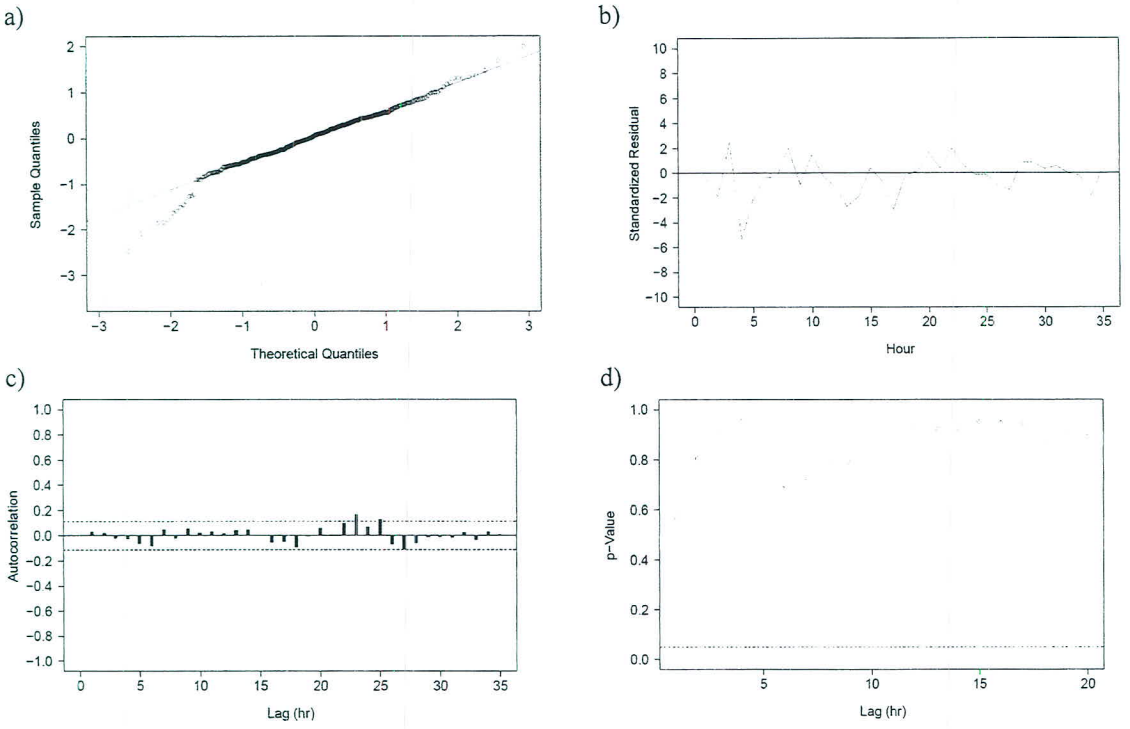

Figure 4.3: Residual diagnostics for the March ARIMA model: (a) Q-Q plot, (b) residuals against time, (c) residual autocorrelogram, and (d) *p*-values for Ljung-Box statistic

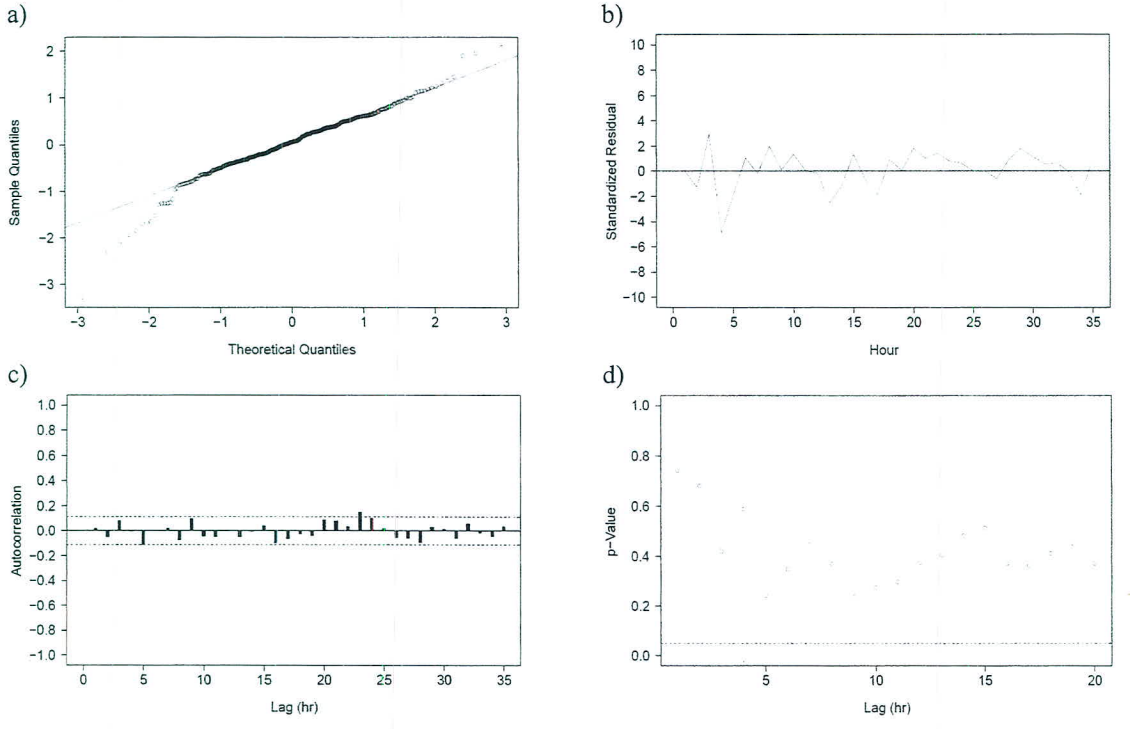

Figure 4.4: Residual diagnostics for the March dARIMA model: (a) Q-Q plot, (b) residuals against time, (c) residual autocorrelogram, and (d) *p*-values for Ljung-Box statistic

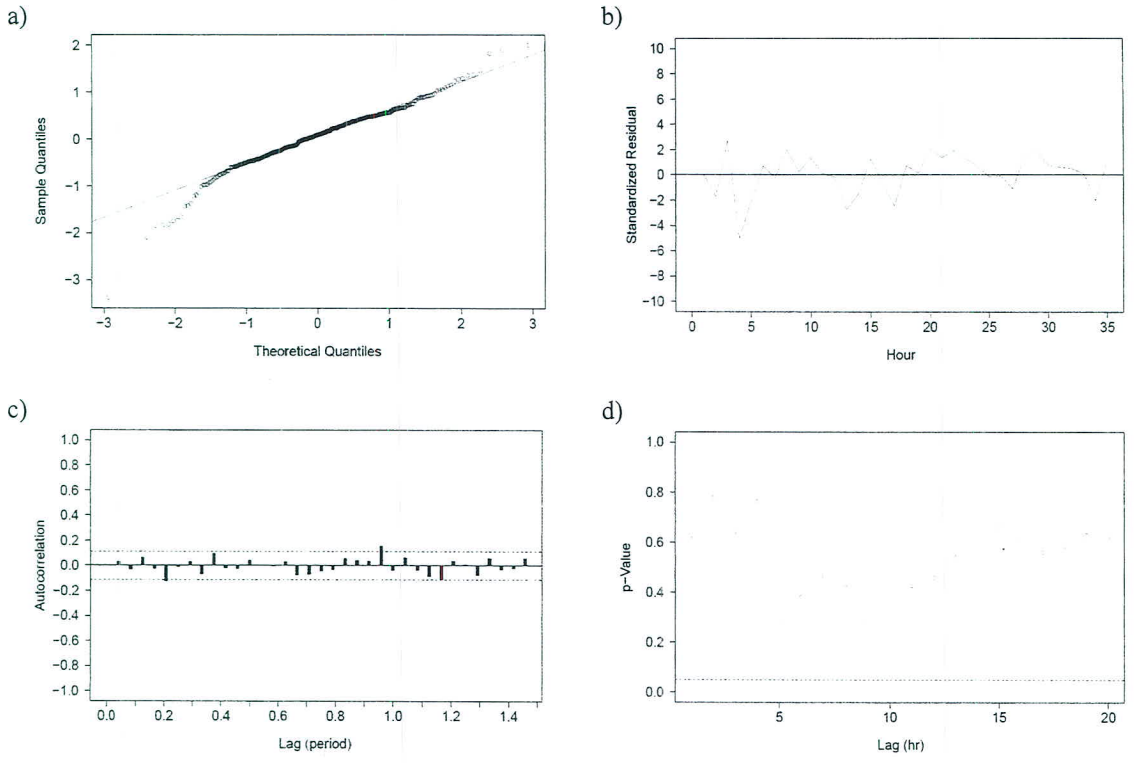

Figure 4.5: Residual diagnostics for the March SARIMA model: (a) Q-Q plot, (b) residuals against time, (c) residual autocorrelogram, and (d) *p*-values for Ljung-Box statistic

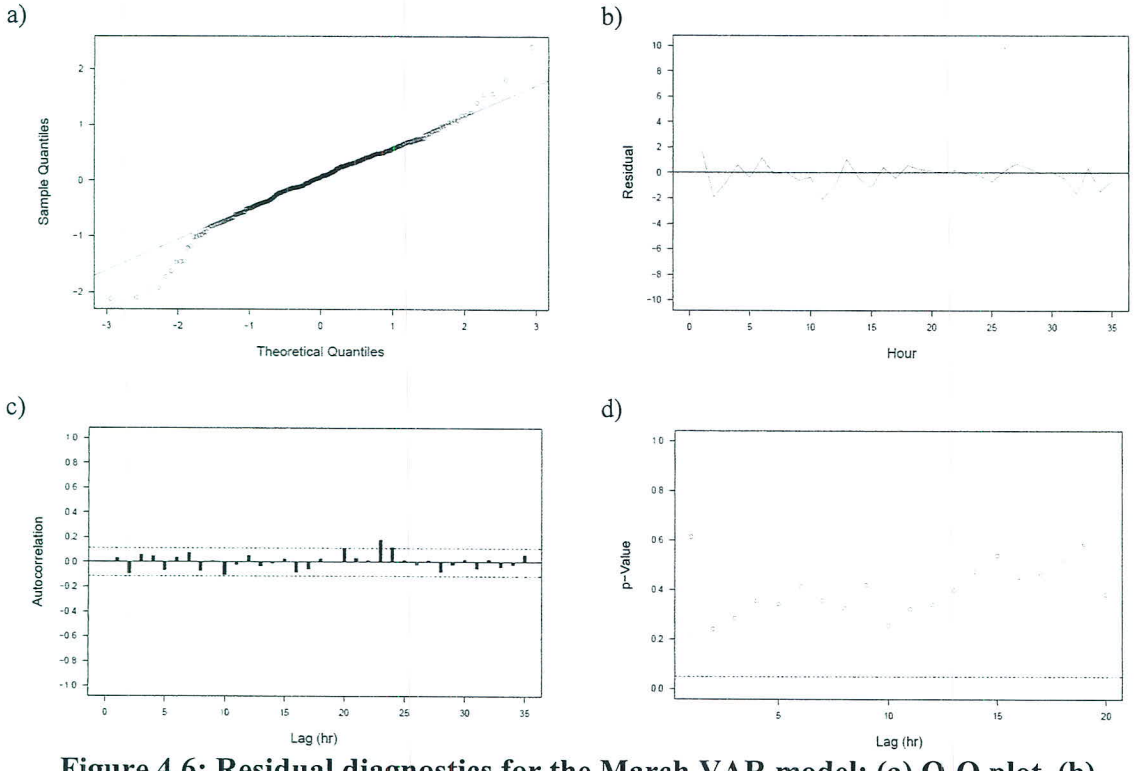

Figure 4.6: Residual diagnostics for the March VAR model: (a) Q-Q plot, (b) residuals against time, (c) residual autocorrelogram, and (d) *p*-values for Ljung-Box statistic

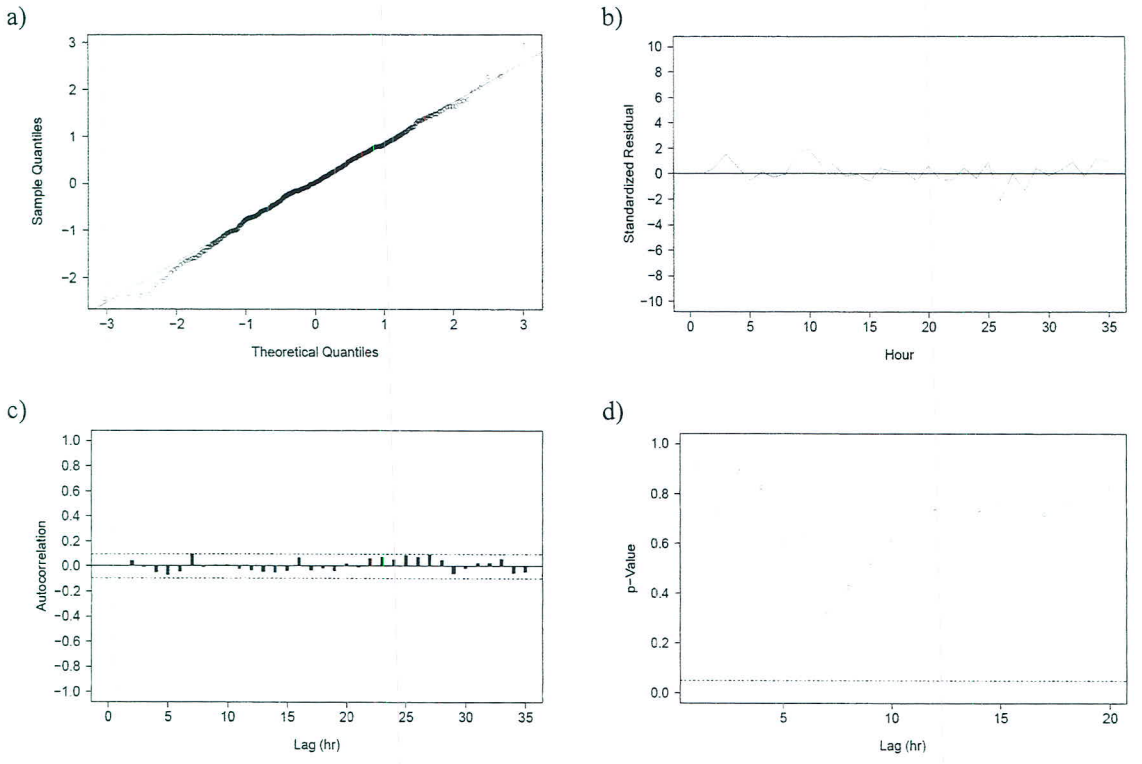

Figure 4.7: Residual diagnostics for the August ARIMA model: (a) Q-Q plot, (b) residuals against time, (c) residual autocorrelogram, and (d) *p*-values for Ljung-Box statistic

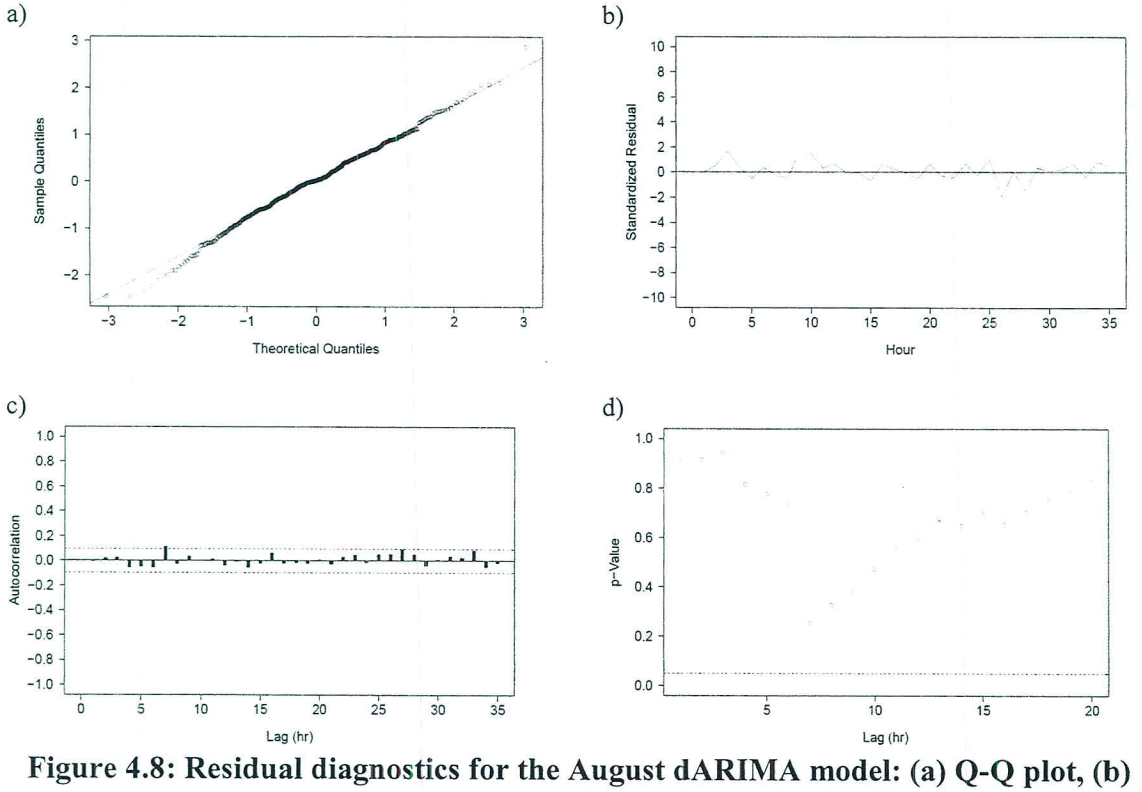

Figure 4.8: Residual diagnostics for the August dARIMA model: (a) Q-Q plot, (b) residuals against time, (c) residual autocorrelogram, and (d) *p*-values for Ljung-Box statistic

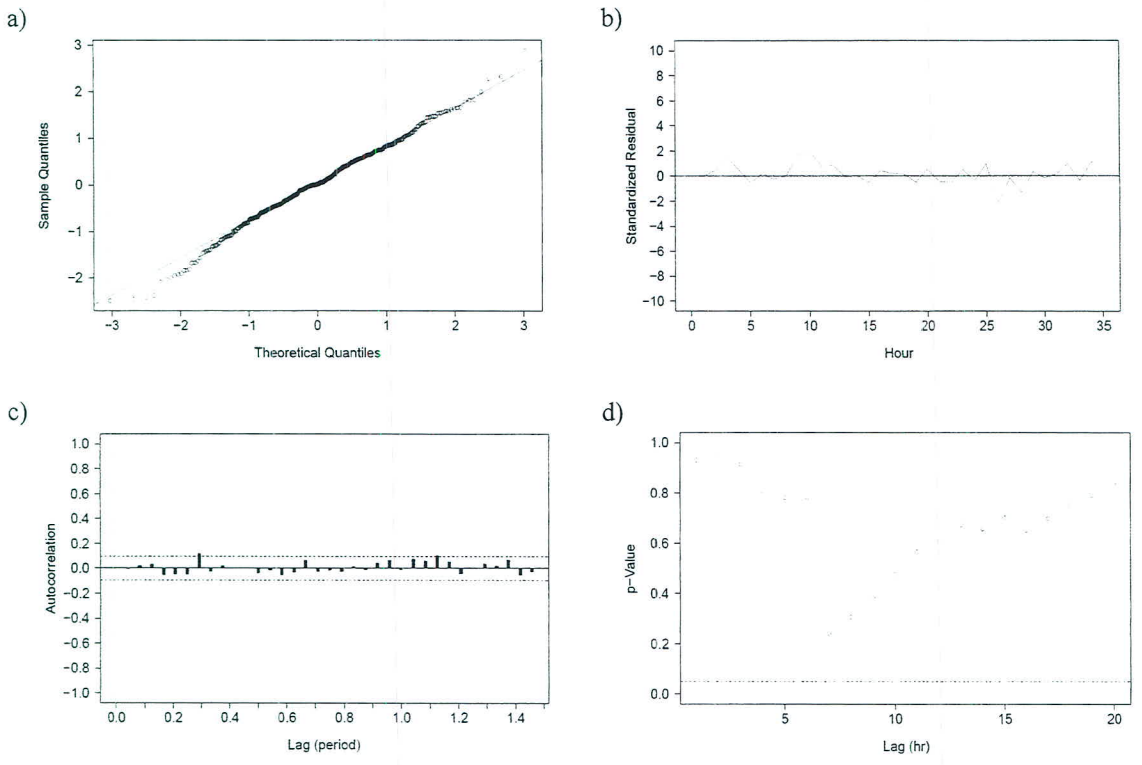

Figure 4.9: Residual diagnostics for the August SARIMA model: (a) Q-Q plot, (b) residuals against time, (c) residual autocorrelogram, and (d) *p*-values for Ljung-Box statistic

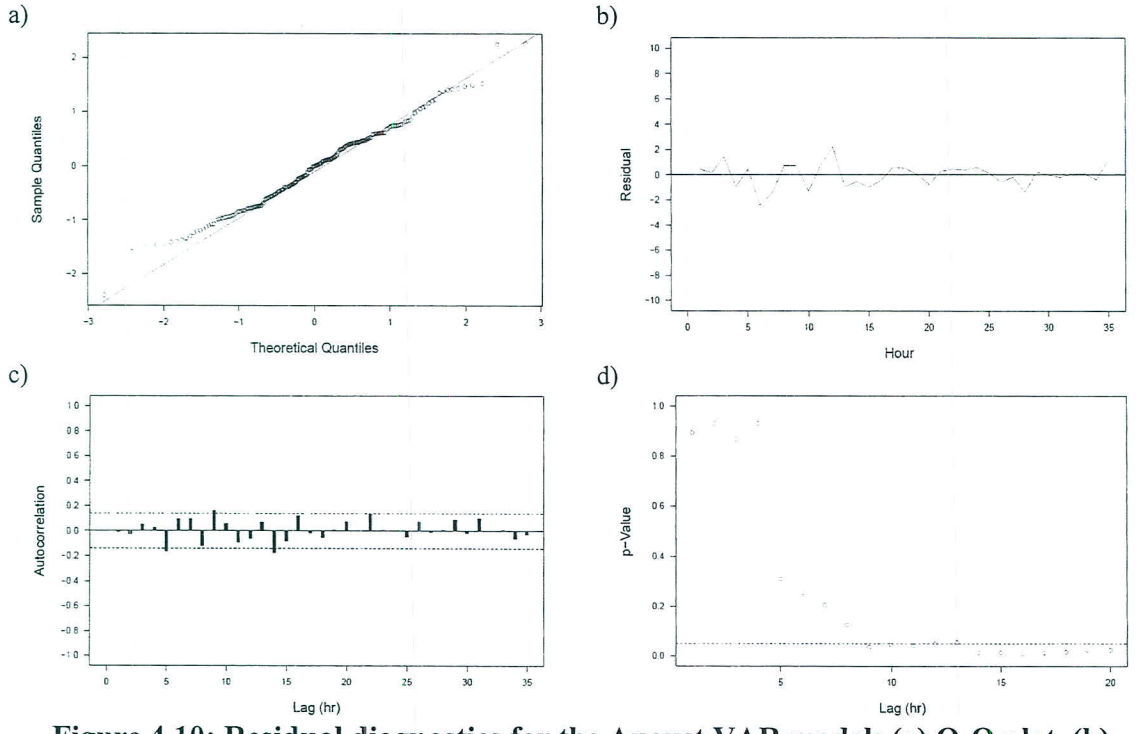

Figure 4.10: Residual diagnostics for the August VAR model: (a) Q-Q plot, (b) residuals against time, (c) residual autocorrelogram, and (d) p-values for Ljung-Box statistic

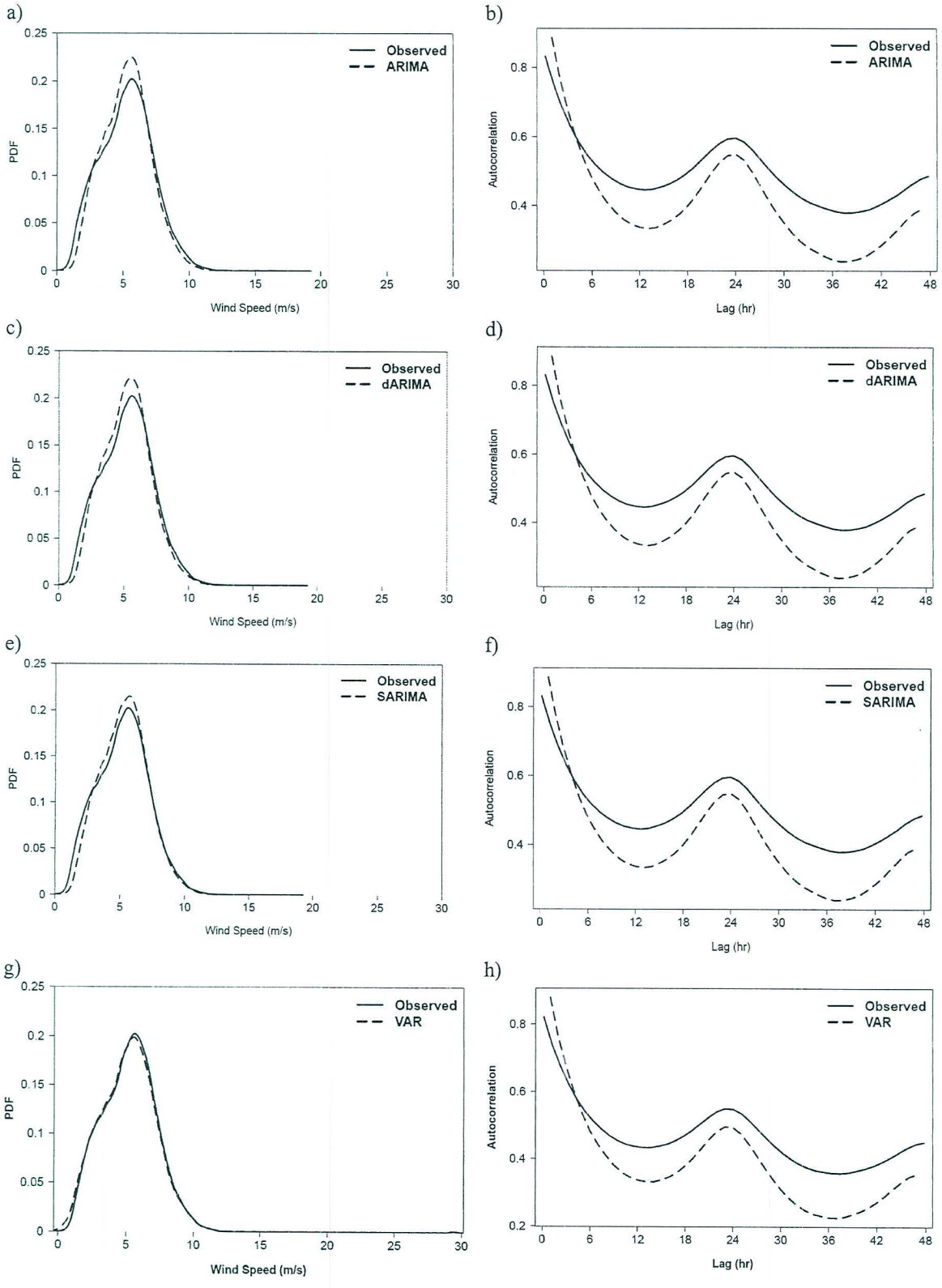

Figure 4.11: The comparison of probability density functions and sample autocorrelations of observed and fitted wind speed series

4.3 Forecast evaluation

In assessing the prediction performance of all models, wind speed is considered as the main variable. As mentioned previously, the evaluation is carried out by means of statistical metrics such as mean error (ME), skill score (SS), centered root mean square error (CRMSE) and correlation coefficient (ρ). Figures 4.12-4.15 show example forecasts from some episodes in the months of March and August. The forecasts from each episode are compared to the corresponding observations for the 100-m wind speed data at PCD-M2 for each month and for the entire validation period (see Figures 4.16 and 4.17). As seen, the performance varies for all models, and no single model was found to be superior to the rest in all cases. In terms of monthly ME, PS is outperformed by ARIMA, dARIMA, SARIMA, and VAR in all months, with dARIMA and VAR being best in 4 months each. The VAR model was based on wind speed, vertical temperature difference and land-sea temperature contrast. SARIMA performs best in 2 months. dARIMA and VAR perform comparably with monthly ME ranging from 1.06-1.67 m s^{-1} and 1.03-1.83 m s^{-1} respectively. For PS and ARIMA, the monthly ME ranges from 1.39-2.25 m s^{-1} and 1.10-1.71 m s^{-1} respectively. Considering the whole period, the ME is the highest for PS at 1.77 m s^{-1}, with dARIMA having the lowest at 1.29 m s^{-1}.

In order to put the performance metrics in a better perspective, Table 4.4 and Figure 4.16 (b) shows the magnitude of the ME with respect to the monthly average wind speed for the validation period for the models. In the table, the relative monthly ME for PS and SARIMA are 22-46% and 19-30% respectively. ARIMA and dARIMA have their relative MEs ranging from 19-30% and 18-32% respectively, while that for the VAR model being 18-30%. In terms of correlation (Figure 4.17 (b)), the results seem to be mostly in agreement with the performance evaluation based on ME. The correlation ranges from 0.21-0.68 for different months and models. On an annual basis, every model achieves correlation of 0.52 or higher with dARIMA having the highest value (≈0.6). For May-August, November and December, dARIMA and SARIMA show relatively good performance (>0.5) in terms of correlation (see Tables B1 and B2). The VAR model performs better in 5 months (February-April, July and September). It was seen that the de-diurnalization treatment on the input detrended series in dARIMA and VAR reflects a simple remedy in dealing with strong diurnality and leads to improved performance. In

terms of skill score (Figure 4.17 (a)), the time series models have better performance in January-May, and have reasonable positive overall merit over PS for all the months. As mentioned previously in the section for forecast evaluation, the skill score can be used to compare different forecasting applications or models.

Considering the hour-dependent performance over the forecast horizon (Figure 4.18), for the entire validation period, it can be seen that the time series models perform better than the persistence model (PS) from 2 hours into the horizon. However, PS levels out with the models towards the end of the horizon. The time-series models seem to be closely matched along the horizon, with no clear advantage to any specific model. The accuracy of the predictions reduces as the window moves away from the last observed point, and therefore, it may be valid to consider only very short-term forecasts. dARIMA, SARIMA and VAR perform reasonably over the first six hours of the time horizon with the percent of ME with respect to the mean wind speed being less than 25%. The ME is within 25% with respect to mean wind speed for the forecast window of six hours in all months except for October and November. The improvement as per time step of the forecast over PS is 1% for 1 hour in advance and 23-27% for 6 hours ahead in terms of ME relative to mean wind speed, for the overall evaluation period. The improvement over PS for the monthly cases varied from 0-2% for 1 hour time step and 3-27% for 6 hours ahead. Here, it should be noted that the first six hours are considered most important for trading of wind power, maintenance scheduling, and dispatch planning by transmission system operators, and therefore it would be of interest to see how the models perform over such a time span. The monthly performance over the forecast horizon is shown in Figure B1, which is agreement with the results seen from the skill score (SS), where for the months of June, July, and August where PS is closely matching the other models. This could be partially attributed to the months being in the southwest monsoon where there are regular westerly and south-westerly winds, and also strong gusts as seen from Table 3.1, where August is seen to have the maximum recorded value of wind speed.

As for the question of how well the models perform with respect to varying magnitude of wind speed (Figure 4.19), it was found that it was more difficult to forecast very low wind speeds (<2 m s^{-1}) and very large wind speeds (>10 m s^{-1}). Therefore, for the months

(June-August) with relatively higher mean wind speed and gusts, the performance of the time series models will be poor. The Taylor diagram (Figure 4.20) shows the overall performance of the time-series models where the model which lies closest to the reference point corresponding the observed data is considered the best. In this case, SARIMA and dARIMA appear closer than the other models and this in agreement with the results earlier discussed. The monthly Taylor diagrams (Appendix B) are also indicative of the results as shown in Figures 4.16 and 4.17. Figure B3 shows the performance for different specifications of the VAR model. This involved varying the number of variables with wind speed as the main variable. It was found out that the VAR model based on wind speed, vertical temperature difference and land-sea temperature difference had slightly better performance than the other VAR specifications. In another study carried out for an on-hill site in Nakhon Ratchasima Province (Figure B4), SARIMA was found to have better performance than the ARIMA and dARIMA models (Kaigwara and Manomaiphiboon, 2013).

(Intentionally left blank)

Table 4.4: Monthly performance of models in terms of ME ($m\ s^{-1}$) and its relativity (%) with respect to monthly mean wind speed

	Mean	PS		ARIMA		dARIMA		SARIMA		VAR	
		ME	%	ME	%	ME	%	ME	%	ME	%
Jan.	4.89	2.25	46	1.40	29	1.42	29	1.36	28	1.42	29
Feb.	5.65	1.68	30	1.17	21	1.09	19	1.10	19	1.10	19
Mar.	5.71	1.65	29	1.10	19	1.06	19	1.10	19	1.03	18
Apr.	4.94	1.82	37	1.27	26	1.21	24	1.25	25	1.15	23
May	5.38	1.91	36	1.36	25	1.31	24	1.33	25	1.43	27
Jun.	6.39	1.56	24	1.29	20	1.24	19	1.24	19	1.56	24
Jul.	6.28	1.57	25	1.31	21	1.26	20	1.30	21	1.34	21
Aug.	6.32	1.39	22	1.23	19	1.15	18	1.21	19	1.23	19
Sep.	5.09	1.78	35	1.44	28	1.32	26	1.40	28	1.21	24
Oct.	5.70	1.86	33	1.59	28	1.33	23	1.33	23	1.57	28
Nov.	5.22	1.76	34	1.57	30	1.67	32	1.59	30	1.55	30
Dec.	7.04	2.07	29	1.71	24	1.50	21	1.48	21	1.88	27
All	5.72	1.77	31	1.36	24	1.29	23	1.31	23	1.37	24

a)

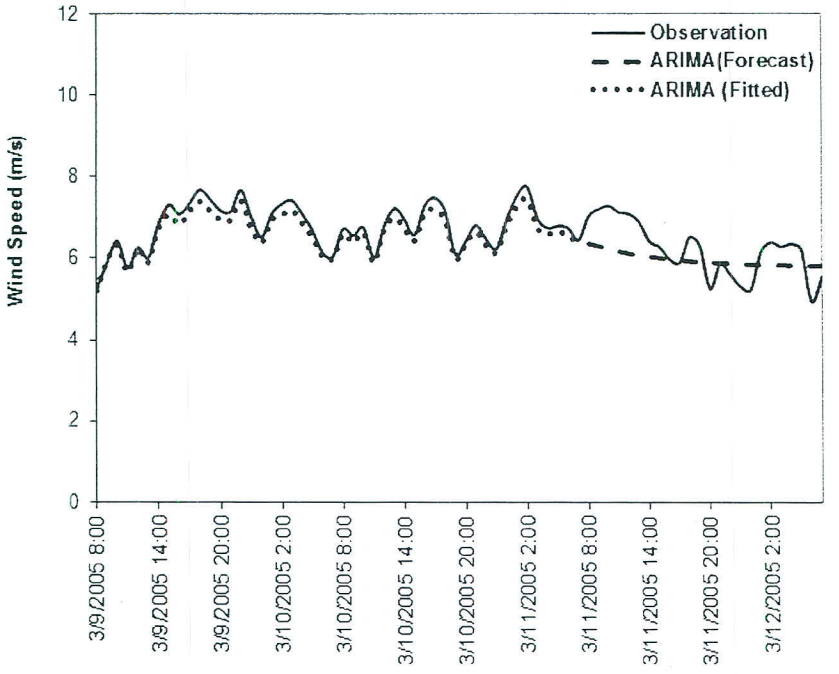

b)

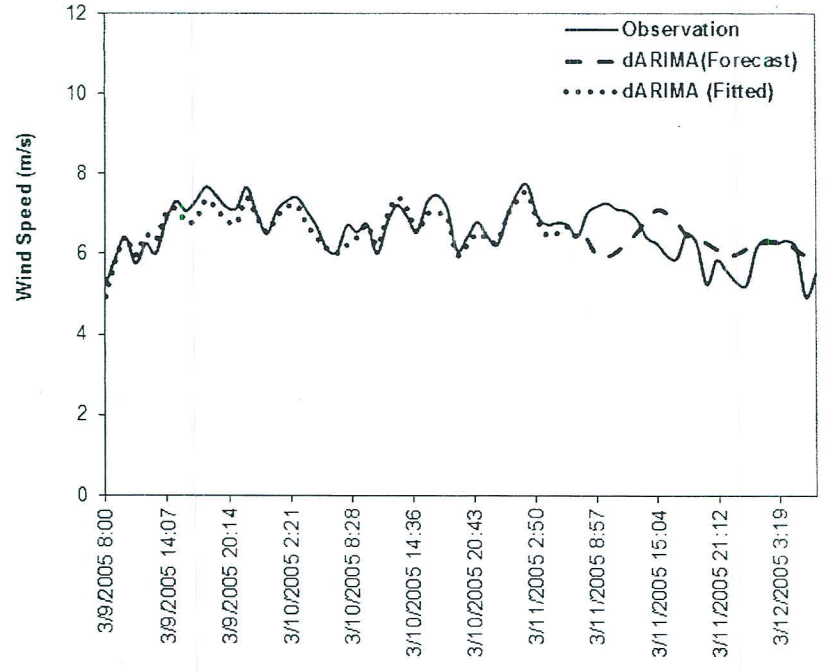

Figure 4.12: Observations, fitted values and forecasts for (a) ARIMA and (b) dARIMA in March 9-12, 2005

a)

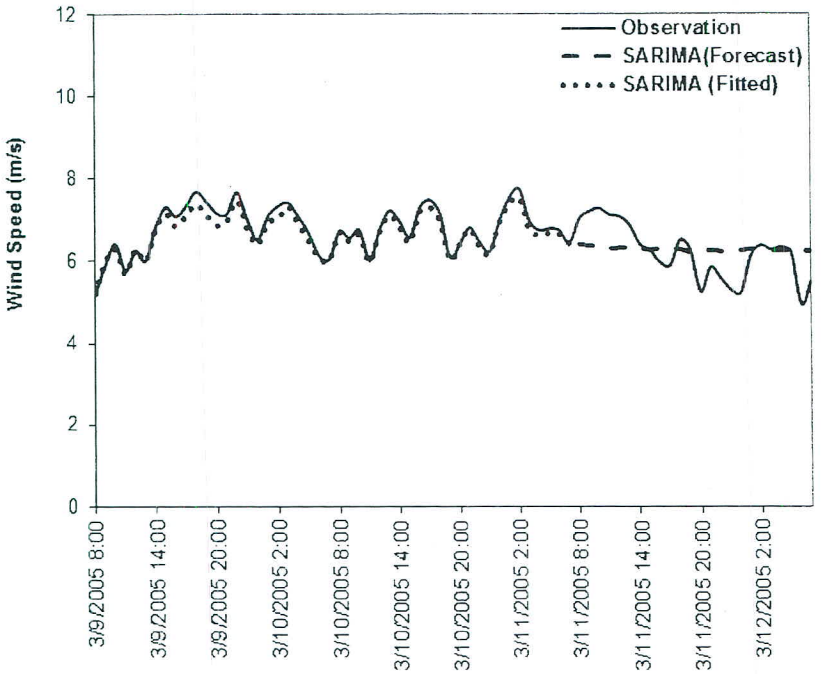

b)

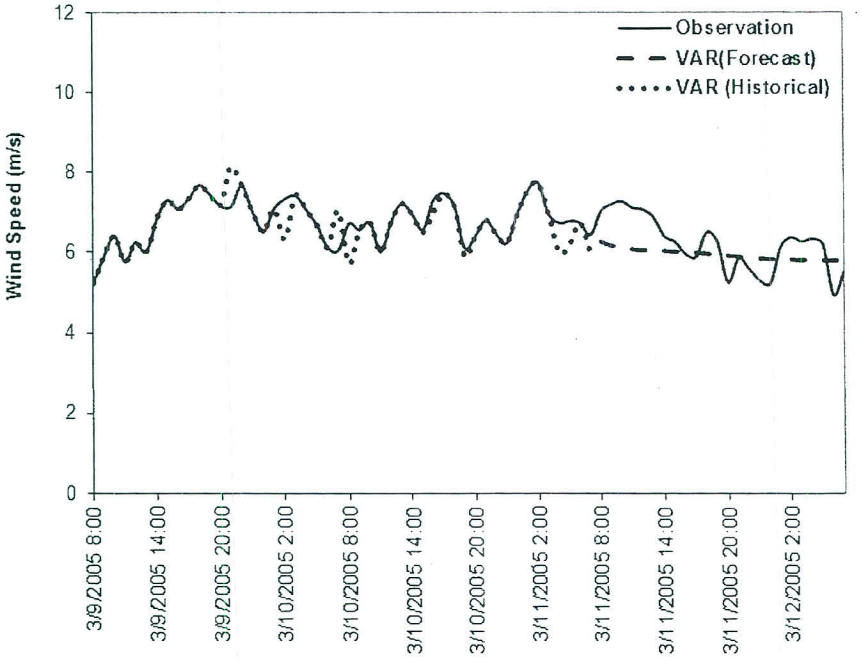

Figure 4.13: Observations, fitted values and forecasts for (a) SARIMA and (b) VAR in March 9-12, 2005

a)

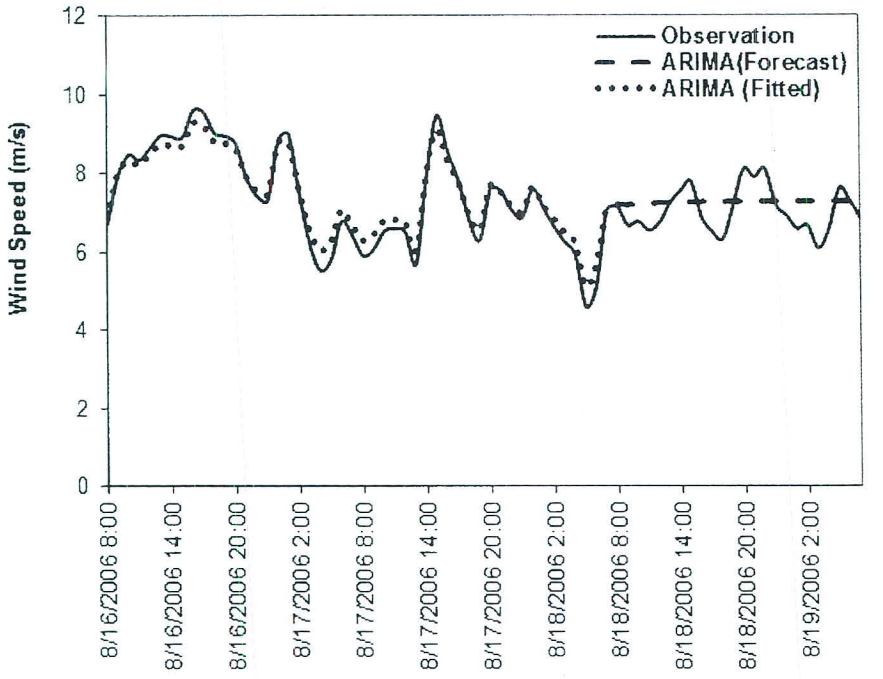

b)

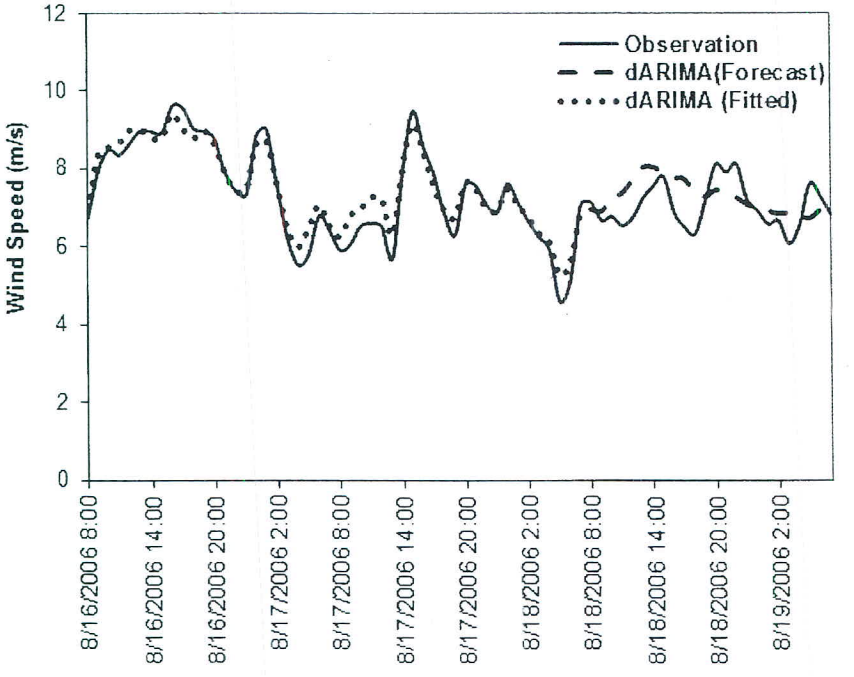

Figure 4.14: Observations, fitted values and forecasts for (a) ARIMA and (b) dARIMA in August 16-19, 2006

a)

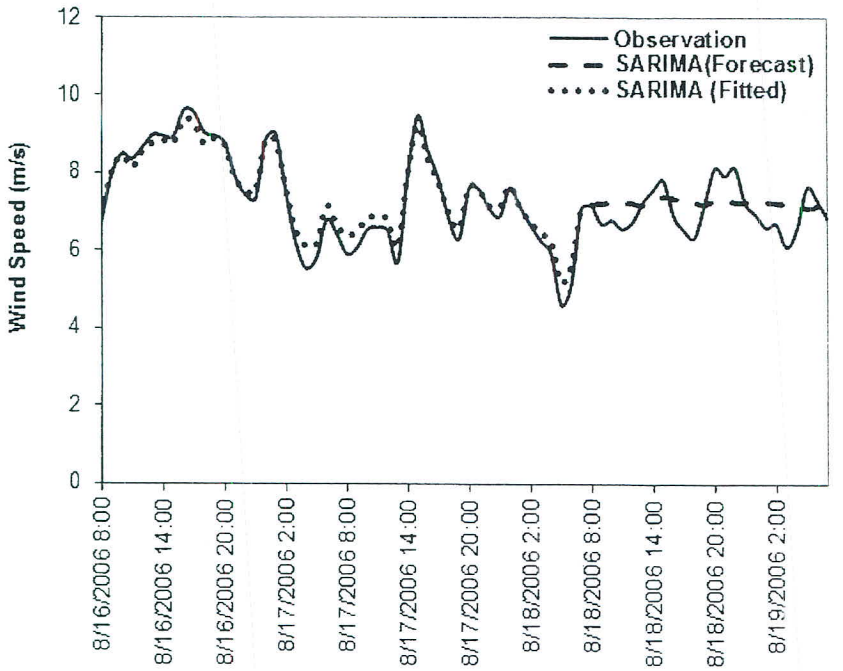

b)

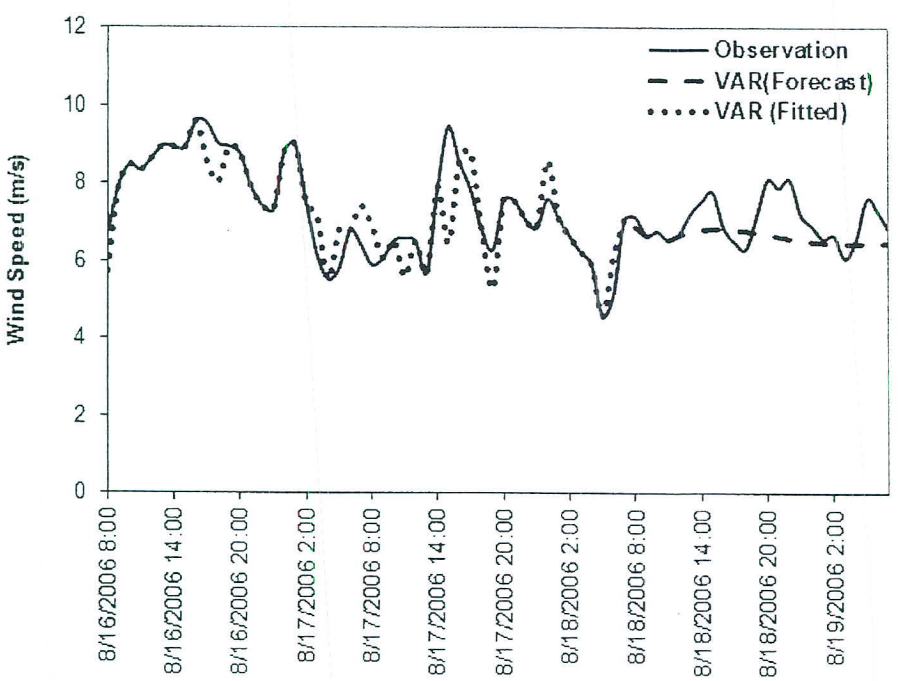

Figure 4.15: Observations, fitted values and forecasts for (a) SARIMA and (b) VAR in August 16-19, 2006

a)

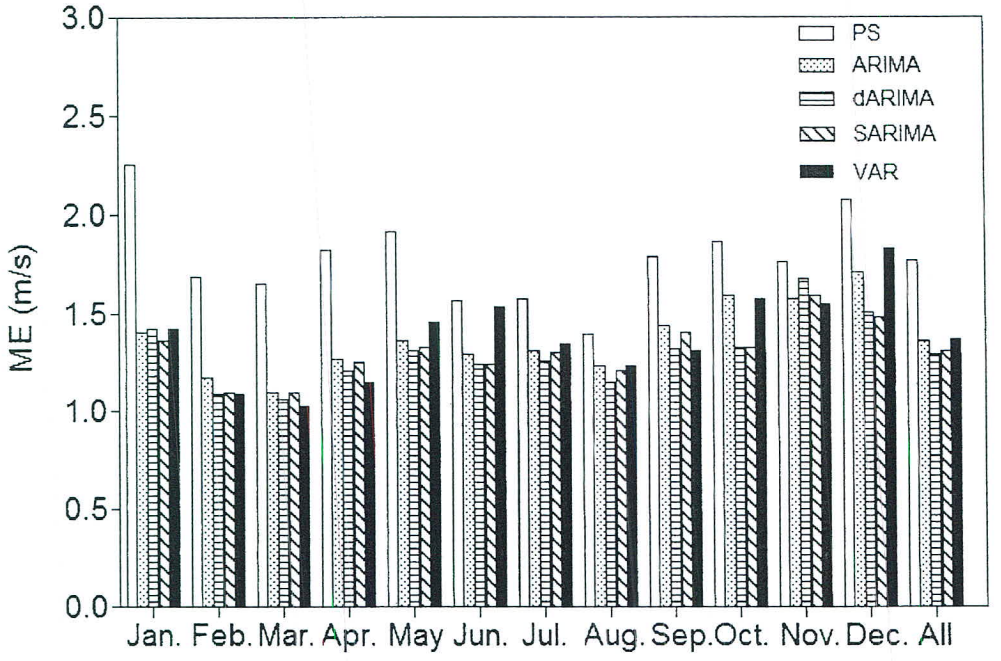

b)

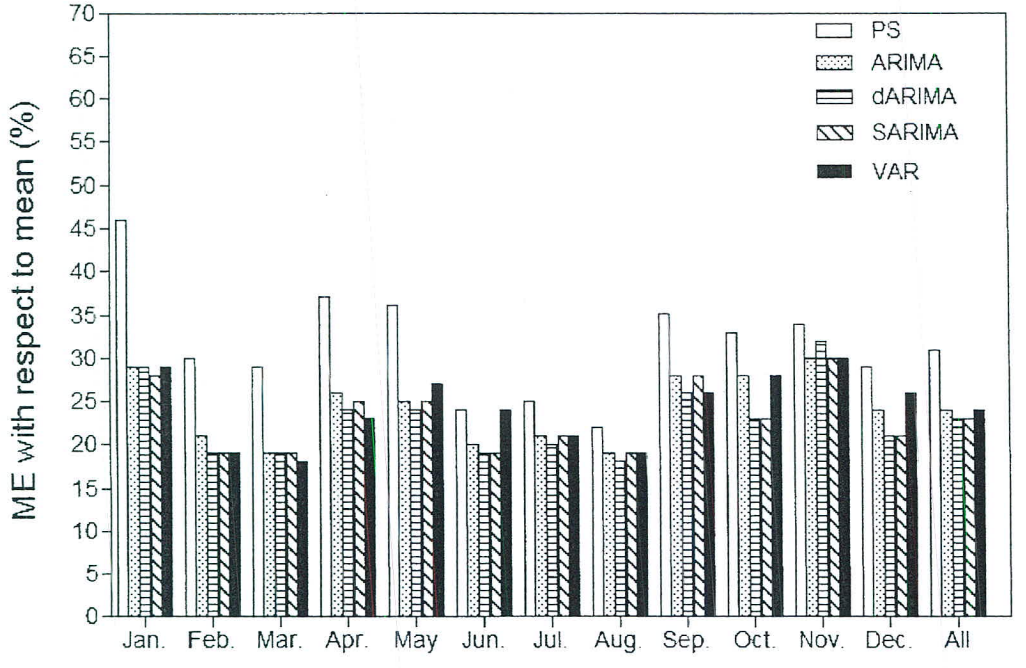

Figure 4.16: (a) ME and (b) percentage of ME with respect to mean wind speed for the selected models

a)

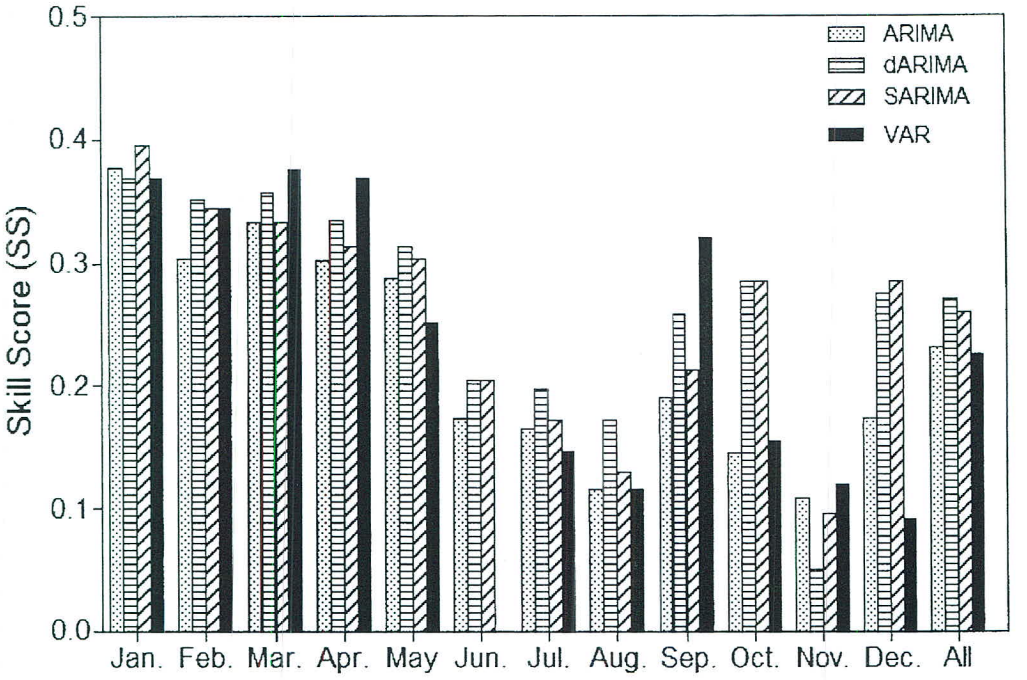

b)

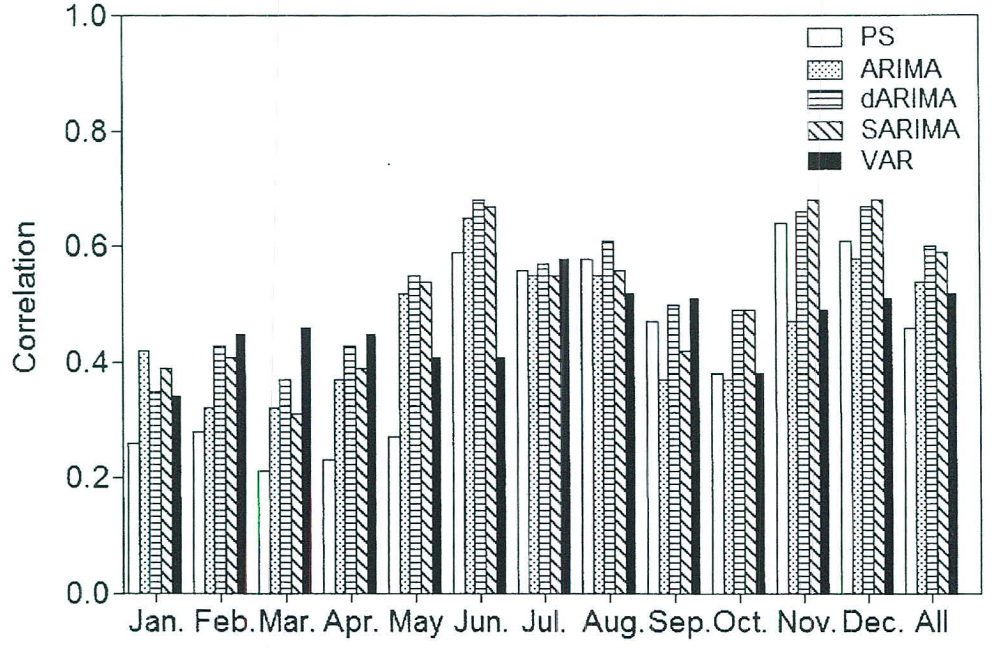

Figure 4.17: (a) Skill score and (b) correlation for the selected models

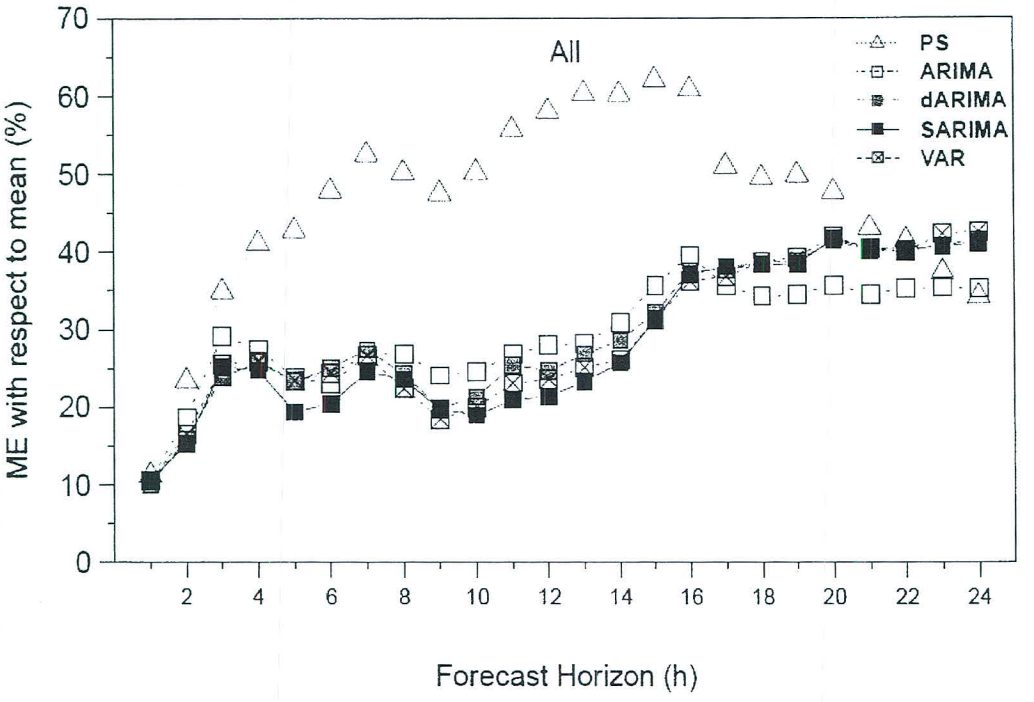

Figure 4.18: Percentage of ME with respect to mean over forecast hours, based on all forecast episodes

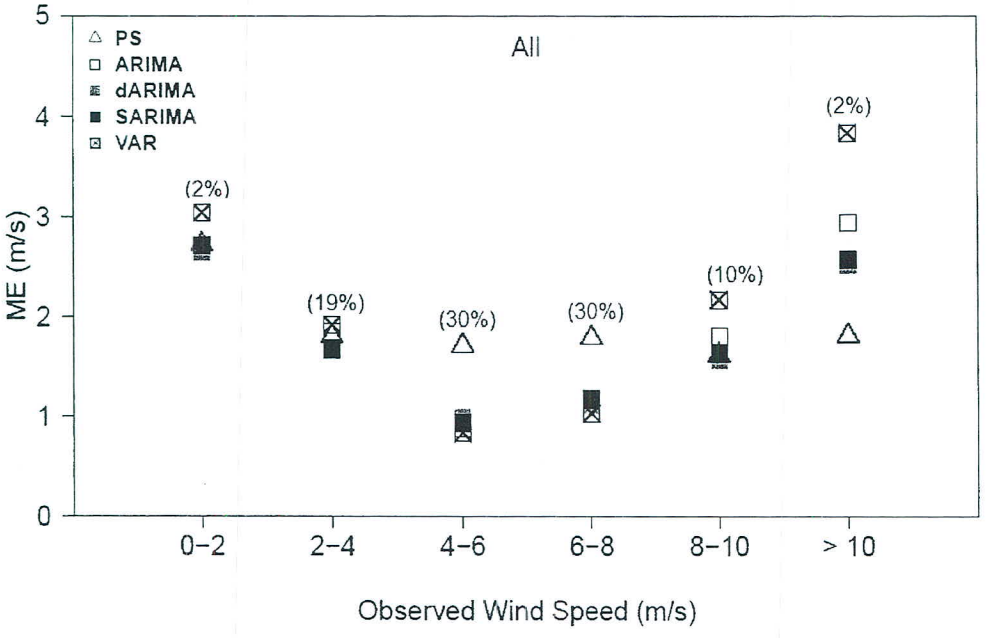

Figure 4.19: ME values by different models over entire evaluation period at different wind speed intervals. Each parenthesized percentage represents the ratio of no. of hours in a particular interval to all hours

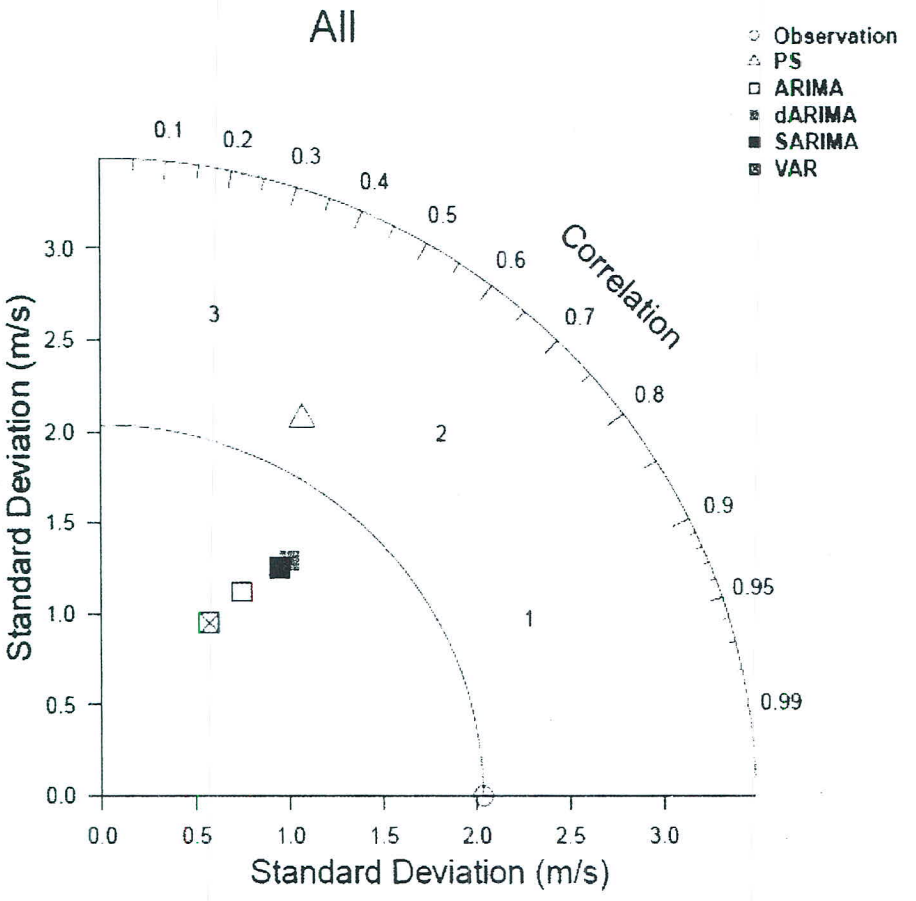

Figure 4.20: Taylor diagram for the selected models based on evaluation period